Design, synthesis, docking, QSAR, ADME studies and pharmacological evaluation of biphenyl-2-oxadiazoles as anti-inflammatory agents

Sujit G. Bhansali and Vithal M. Kulkarni*

Department of Pharmaceutical Chemistry, Poona College of Pharmacy, Bharati Vidyapeeth University, Pune, Maharashtra, India

_____

ABSTRACT

Various 2-(4'-methylbiphenyl-2-yl)-5-aryl-1,3,4-oxadiazole analogues were designed by rational drug design methods. These were synthesized by conventional and microwave assisted methods. Structures of synthesized compounds were confirmed by IR, ^{1}H-NMR, mass and elemental analysis. Compounds were further evaluated for analgesic and anti-inflammatory activity by in vivo models. The synthesized compound VMSB 2, VMSB 4, VMSB 6, VMSB 8, VMSB 11, VMSB 12 and VMSB 14 exhibited significant analgesic and anti-inflammatory activities comparable to standard drug. Also, these compounds showed little ulcerogenic effect compared to standard drug. Docking studies were carried out to understand the binding mode of designed compounds with the COX-2 enzyme. From the docking study, it was observed that ligands bind to the hydrophobic clamp formed by the residues Arg120, Tyr355, Tyr385 and Trp387 which play an important role for COX-2 inhibition. Further, a two dimensional quantitative structure-activity relationship (2D-QSAR) model was obtained using multiple linear regression (MLR) analysis. The pharmacokinetic parameters were calculated for the synthesized compounds and were found to be within the acceptable range defined for human use revealing their potential as possible drug-like compounds. Hence, the results obtained indicated that these compounds can serve as good leads for further modification and optimization.

Keywords: 1,3,4-Oxadiazole; Anti-inflammatory agents; Docking; ADME; QSAR Studies

_____

INTRODUCTION

Nonsteroidal anti-inflammatory drugs (NSAIDs) are widely used for the treatment of pain, fever and inflammatory diseases such as rheumatoid arthritis and osteoarthritis. Conventional NSAIDs inhibit cyclooxygenase (COX) enzymes which catalyze the formation of prostaglandins (PGs) from arachidonic acid. The discovery of COX-2 isoform in the 1990s led to the development of a new class of NSAIDs known as selective COX-2 inhibitors [1]. COX-2 is induced in response to pro-inflammatory conditions, while COX-1 is constitutive and responsible for the maintenance of physiological homeostasis, such as gastrointestinal integrity and renal function. Selective inhibition of COX-2 provides a new class of anti-inflammatory agents with significantly reduced side effects such as gastrointestinal ulcer and renal dysfunction. As a consequence, several selective COX-2 inhibitors such as celecoxib, rofecoxib, valdecoxib and etoricoxib have been developed. However, the recent market withdrawal of rofecoxib due to adverse cardiovascular side effects has raised the concern of safety of selective COX-2 inhibitors [2]. Therefore; there is a need to find new selective COX-2 inhibitors with improved safety profile. Nevertheless, the potential therapeutic applications of selective COX-2 inhibitors have been expanded beyond the areas of analgesia and inflammation, as shown by recent studies on COX-2 that have been focused on cancer and neurodegenerative disorders [2].

Recently, a novel series of 1,3,4-oxadiazoles based derivatives were reported [3] and subjected to anti-inflammatory, analgesic activity and molecular docking studies to target COX-2 enzyme and were found to be potent COX-2

156

_____

inhibitor. Also, synthesis, COX-2 inhibitory potential, and antiinflammatory activity of pyrazole substituted 1,3,4-oxadiazoles and 1,2,4-oxadiazoles were reported [4]. Our studies and of other researchers [3,4] have shown that derivatization of the carboxylate function of some NSAIDs resulted in an increased anti-inflammatory activity with a reduced ulcerogenic effect. Hence, it is not irrelevant to speculate that replacing the terminal carboxylic function of NSAIDs by oxadiazole ring, a five membered heterocyclic nucleus, may enhance the anti-inflammatory activity of such compounds. Hence, by incorporating the oxadiazolyl moiety, we hope to get a better anti-inflammatory molecule. In our laboratory biphenyl scaffold was conceived to possess anti-inflammatory activity [5, 6]. Several research articles were published on the same and a U.S. patent was obtained [7].

Based on these findings, a novel series of biphenyl analogues were designed and synthesized. These compounds possessed biphenyl as the basic nucleus and analogues were prepared at the carboxylic function to obtain several oxadiazoles. To investigate the detailed intermolecular interaction between designed ligand and the targeted enzyme, automated molecular docking software Glide was used for docking study of these molecules on COX-2 enzyme. According to the docking scores obtained from Glide software, designed molecules were further optimised and synthesized. Preliminary anti-inflammatory activity was screened by *in vivo* studies.
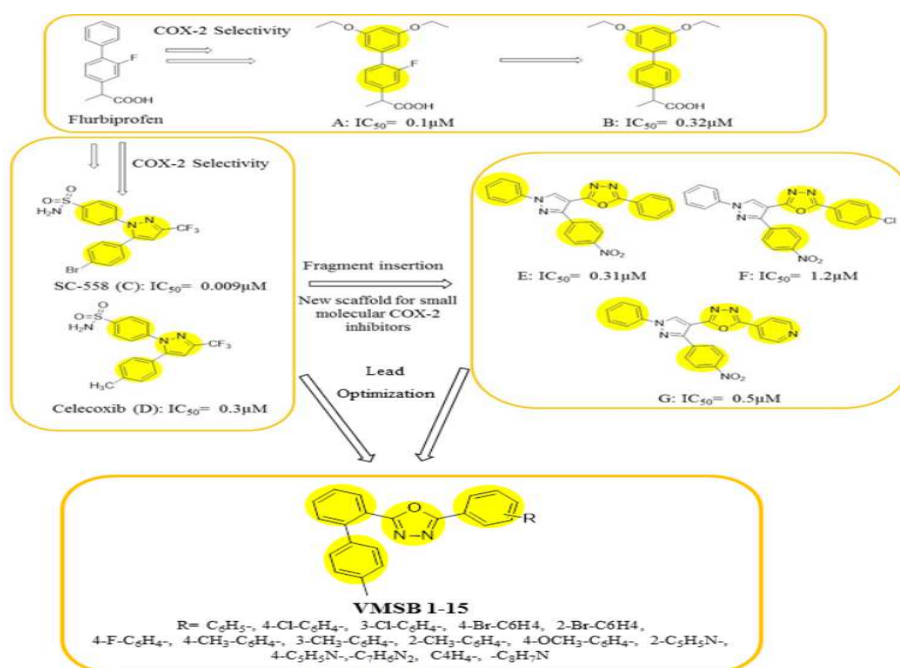

**Figure 1 Representative examples of selective COX-2 inhibitors (A–G) [8-19]**

## MATERIALS AND METHODS

2.1. Materials

All the chemicals were procured from commercial sources such as Sigma-Aldrich, Merck and Loba Chemie and were purified prior to use. All the fifteen derivatives were synthesized in our laboratory. The melting points of synthesized compounds were taken on Veego VMP - D digital melting point apparatus by open capillary method and are uncorrected. The reaction completion was monitored by thin layer chromatography on Merck pre coated silica gel F_{254} plates. TLC plates were visualized using iodine chamber or observed under UV light. Fourier transform infrared (FT-IR) spectra were recorded in potassium bromide (KBr) disk on "Jasco FTIR 4100" and are reported in cm^{-1}. Proton nuclear magnetic resonance (^{1}H-NMR) spectra were recorded in $CDCl_3$/ DMSO-D_6 using "Bruker Avance (400 MHz) with tetra methyl silane (TMS) as an internal standard. The mass spectra of compounds were recorded on Agilent 6460 Triple Quadrupole LC/MS System with Jet stream ESI ion source. Elemental analysis of compounds was detrmined on vario MICRO V2.0.3, Elementar analysis system GmbH.

_____

2.2. Synthetic scheme of designed compounds
2.2.1.Step 1: Synthesis of 4'-methyl-[1,1'-biphenyl]-2-carbohydrazide

4'-methyl-[1,1'-biphenyl]-
2-carboxylic acid

1   2

4'-methyl-[1,1'-biphenyl]-2-
carbohydrazide
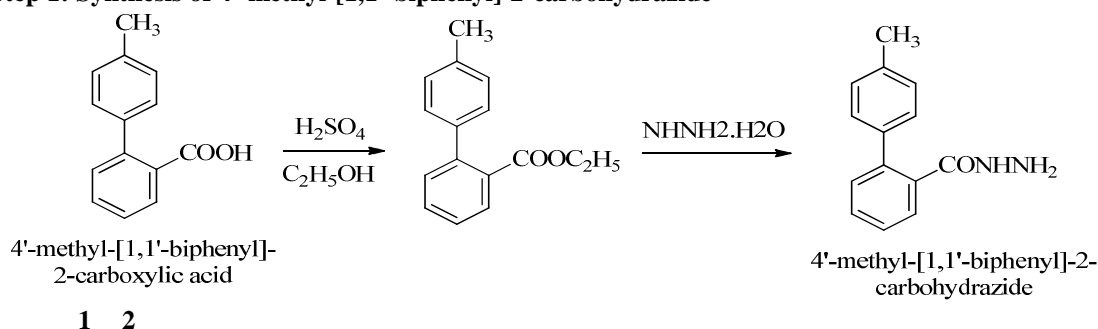
2.2.2.Step 2: Synthesis of 2-(4'-methylbiphenyl-2-yl)-5-aryl-1,3,4-oxadiazole derivatives

4'-methyl-[1,1'-biphenyl]-2-carbohydrazide

2   VMSB 1-15

2-(4'-methylbiphenyl-2-yl)-5-aryl-
1,3,4-oxadiazole derivatives
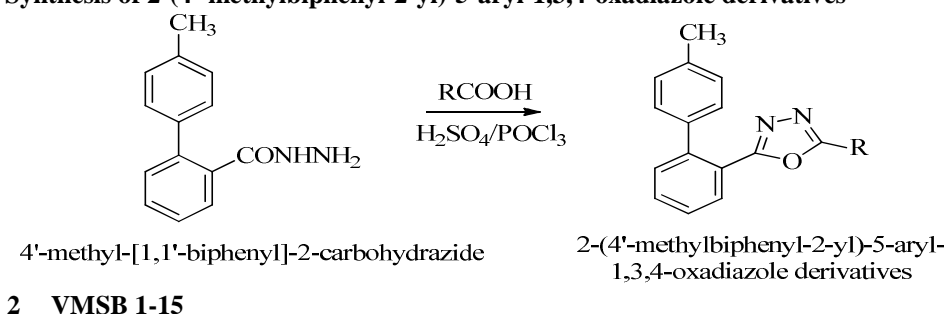
2.3. Procedure for synthesis of 4'-methyl-[1,1'-biphenyl]-2-carbohydrazide (2):
2.3.1.Conventional Synthesis
2.3.1.1. Step 1
A solution of the 4'-methyl-[1,1'-biphenyl]-2-carboxylic acid (10 mmol), absolute ethanol (10 ml) and concentrated sulfuric acid (1 ml) was heated under reflux for 4-5h. The solvent was evaporated under reduced pressure, the remaining contents cooled to room temperature, neutralized with a concentrated solution of sodium carbonate; the aqueous solution was extracted with chloroform (3 × 20 ml). The combined chloroform extracts were dried, and the solvent was removed under reduced pressure to yield the corresponding ethyl ester. The B.P. was found to be 120°C and the yield was found to be around 80-85%.

2.3.1.2. Step 2
Hydrazine hydrate (80%, 11 mmol) and ethyl ester (10 mmol) formed in the step 1 were taken in a round bottomed flask. Small amount of ethanol was added to make the reaction-mixture a clear solution. The contents were refluxed for 3-5 hr. The progress of the reaction was monitored by thin layer chromatography. After completion of the reaction, the ethanol was distilled off under reduced pressure to give the 4'-methyl-[1,1'-biphenyl]-2-carbohydrazide (**2**). The hydrazide was recrystallized using ethanol. The hydrazides were characterized on the basis of physiochemical and spectral data. The reaction time by conventional method of Step 1 and Step 2 for the synthesis of 4'-methyl-[1,1'-biphenyl]-2-carbohydrazide (**2**) was 15-28 h, with overall yields of 64-86%.

2.3.2.Microwave assisted synthesis
A mixture of hydrazine hydrate (80%, 2.5 mmol) and the 4'-methyl-[1,1'-biphenyl]-2-carboxylic acid (**1**) (1 mmol) was irradiated in closed vessel under microwave irradiation at 300W and 250 °C, with 250 psi maximum pressure. The reaction was complete within 7 minutes. The reaction mixture was cooled; the separated solid was filtered, dried and crystallized from ethanol to give the corresponding 4'-methyl-[1,1'-biphenyl]-2-carbohydrazide (**2**) in 90-94% yields.

2.3.3.Solvent Free Synthesis (Grinding Technique)
The 4'-methyl-[1,1'-biphenyl]-2-carboxylic acid (**1**) (1.0 mmol) was ground with hydrazine hydrate (80 %, 3.75 mmol) by a pestle in a mortar for 3-5 minutes and left for digestion (overnight) when the reaction mixture set into a solid mass. The completion of the reaction was checked by thin layer chromatography. The solid mass was crystallized from ethanol to give 4'-methyl-[1,1'-biphenyl]-2-carbohydrazide (**2**) in 80-84% yields.

_____

2.4. Procedure for synthesis of 2-(4'-methylbiphenyl-2-yl)-5-aryl-1,3,4-oxadiazole derivatives (VMSB 1-15):
2.4.1.Conventional Synthesis
A mixture of 4'-methyl-[1,1'-biphenyl]-2-carbohydrazide (**2**) (1 mmol), substituted benzoic acids (1 mmol) and phosphorus oxychloride (2.5 mmol) was refluxed at 100-110°C for 6h or dissolved in sulphuric acid (10mmol) and reaction was continued for 30h at room temperature. The excess solvent was distilled off under reduced pressure and the residue was quenched with ice cold water and neutralized by dilute NaOH solution. The separated solid was filtered, washed and dried. The crude product was purified by recrystallization from a suitable solvent to afford oxadiazoles (**VMSB 1-15**) in 38-42% yield.

2.4.2.Microwave assisted synthesis
The mixture of 4'-methyl-[1,1'-biphenyl]-2-carbohydrazide (**2**) (0.002 mol), aromatic acid (0.003 mol) and phosphorus oxychloride (1 ml) was ground to get a homogeneous mixture and then heated in a beaker under microwave irradiation at 160 W. The reaction was complete within 5-10 min. Completion of the reaction was monitored by TLC. The contents were cooled to room temperature and added to excess ice-cold water. The solid product separated was collected by filtration. Further, purification was done by recrystallization from ethanol-water to give oxadiazoles (**VMSB 1-15**) in 53-62% yield.

2.5.Pharmacological Screening
2.5.1.Acute toxicity study
Adult albino mice of either sex were subjected to acute toxicity studies as per guideline (AOT No. 425) suggested by Organization for Economic Cooperation and Development (OECD) [20]. Doses of 550, 1750, 2000 mg/kg of test compound were administered orally to mice and control group received normal saline 10 ml/kg, p.o. The mice were observed by housing them individually in the polypropylene metabolic cages continuously for 2h for behavioral, neurological and autonomic profiles and for any lethality during next 48h. Use of AOT 425 software was made to obtain higher doses for LD_{50} determination as per OECD guidelines.

2.5.2.Acetic acid-induced abdominal writhing
Pain was induced by injection of irritant (acetic acid) into the peritoneal cavity of mice. The animals react with a characteristic stretching behavior called writhing i.e. contractions of abdomen, turning of trunk and extension of hind limb, which was observed in treated groups of animals. Mice were treated according to the reported method [21]. The animals were divided into seventeen groups (n=6) viz;

Group 1- Acetic acid control,
Group 2- Diclofenac (10 mg/kg, p.o.),
Group 3 to Group 17- Compounds VMSB 1 to 15 (10 mg/kg, p.o.).

The animals were pre-treated orally with test compounds and diclofenac, 60 min before administration of acetic acid (0.9%, intra-peritoneal). The number of abdominal constrictions (full extension of both hind paws) was cumulatively counted over a period of 15 min. The analgesic activity was expressed as mean number of writhes and percent inhibition, which was calculated by following formula:

% Inhibition = [Wc - Wt /Wc] *100

Where, Wc and Wt are mean number of writhes observed in vehicle (control) group and treatment group respectively. (Table 1)

2.5.3.Carrageenan-induced rat hind paw edema
To test the effect of synthesized compounds on acute inflammation, the reported method [22, 23] was used. Female Wistar rats (175-200gm) were used for the experiment. The rats were divided into seventeen groups (n=6) viz;

Group 1- Carrageenan control,
Group 2- Diclofenac (10mg/kg, p.o.),
Group 3 to Group 17 Compounds VMSB 1 to 15 (10mg/kg, p.o.).

The hind paw edema was produced by injecting 0.1 ml of 1% carrageenan in the right hind paw of each rat under the sub-plantar region. Rats were pre-treated with orally administered test compounds and diclofenac 1h before carrageenan injection. The rat pedal volume up to the ankle joint was measured using plethysmometer (Ugo Basile, Italy) at 1, 3, and 5h after the carrageenan injection (time 0 considered). Increase in the paw edema volume was considered as the difference between 1, 3 and 5h and expressed as the mean difference in paw volume (ml). Percent

_____

inhibition of edema volume between treated and a control group was calculated as following formula and result presented in Table 2.

% Inhibition = [Vc - Vt /Vc] *100

Where Vc and Vt represent mean increase in paw volume in control and treated groups, respectively.

2.5.4.Cotton pellet induced granuloma in rats
In order to test the effect of synthesized compounds on chronic inflammation, reported method [24] was used. Female Wistar rats were divided into five groups of 6 rats each.

Group 1: - Vehicle control,
Group 2: - Standard (Diclofenac 10 mg/kg p.o.),
Group 3-5: - VMSB 2, VMSB 11 and VMSB 12 (10 mg/kg, p.o.), respectively.

Chronic inflammation was produced by implanting the pre-weighed sterile cotton pellets (50 mg) in the axilla region of each rat through a small incision. Before implanting the cotton pellets, rats were anaesthetized with anaesthetic ether. VMSB 2, VMSB 11, VMSB 12 and diclofenac were administered orally for seven consecutive days after the cotton pellet implantation.

On the eighth day animals were sacrificed by cervical dislocation and stomach was removed for blind assessment of gastric damage. Cotton pellets were removed from animal's body, freed from the extraneous tissues, dried at 60°C for 24 h and weighed. The severity of the gastric damage was determined for each stomach by the ulcerogenicity studies and histopathology (microscopic examination). The ulcer index for each treatment was calculated.

The severity of ulcers was recorded by the following score scale: 0, no lesion; 1, redness; 2 diffuse, pronounced lesions; 3, severe lesions [25]. Ulcer index (UI) was calculated by following formula:

UI= Overall Score × % of rats with ulcer/ Number of rats treated

2.5.5.Statistical analysis
The data obtained from the above studies was analysed by one way analysis of variance (ANOVA) for determining the significant difference between the groups. The inter group significance or post hoc comparison was analysed using Dunnett's test. P values < 0.05 were considered to be significant. All the values were expressed as percentage inhibition of respective behaviour model relative to control group.

2.6. Docking Studies
In the present study, protein preparation and protein refinement was done using protein preparation wizard and docking study was performed using Glide 5.8 [26] running on Windows 7 Service Pack 1 OS. The crystal structure of COX-2 inhibitor complex with SC-558 was obtained from Protein Data Bank (pdb: 1CX2) [27]. Since the structure is a tetramer with duplicate binding sites, extra binding sites and the associated chains were removed by picking and deleting molecules or chains and only 'C' chain was used for docking study. After importing, a protein is subjected for several structural issues like: assignment of bonds and bond orders, addition of hydrogens, filling in missing side chains, adjusting bonds and formal charges for metals, and correcting mislabelled elements. Prime interface [28] integrated with maestro was used to add the missing residues in side chain. All the water molecules were deleted. H-atoms were added to the protein, including the protons necessary to determine the correct ionization and tautomeric states of amino acid residues. The protein structure minimization was carried out with Impact Refinement module, using the Optimized Potentials for Liquid Simulations (OPLS)-2005 force field to relieve the steric clashes which may exist in the structures. When the Root Mean Square Deviation (RMSD) reached a maximum cut-off of 0.30 Å the minimization was terminated.

Receptor grid generation panel was used to generate the receptor grid. To identify the active site, ligand was selected to define the position and size of active site. The shape and properties of the receptor are represented on a grid by different sets of fields that provide progressively more accurate scoring of the ligand poses. The binding site is outlined through a rectangular box enclosing the translations of the mass centre of the ligand. The Grid-based Ligand Docking with Energetics (Glide) algorithm estimates a systematic search of positions, orientations and conformations of the ligand in the enzyme-binding pocket through a series of hierarchical filters. [29,30]

All the ligands were built using Maestro 9.3 [31] and were prepared using LigPrep 2.5 [32] before docking studies to convert 2D structure to 3D, generate stereoisomer, determine the most probable ionization state at user defined pH,

_____

neutralize charged structures, add hydrogen and to generate the possible number of energy minimized bioactive conformers using ConfGen by applying OPLS–2005 force field. Conformational space was explored through combination of Monte-Carlo Multiple Minimum (MCMM) / Low Mode (LMOD) with maximum number of conformers 1000 per structure and minimization steps 10000. Each minimized conformer was filtered through a relative energy window of 50 kJ/mol and redundancy check of 2Å in the heavy atom positions [33-35].

2.7. QSAR Studies
2.7.1.Software
The QSAR studies were performed on VLife Molecular Design Suite Version 4.8.5 [36] software running on a 2.40 GHz Intel Core i3 processor. All molecules were built in Maestro in Mol2 and were prepared using LigPrep 2.5 [32].

2.7.2.Generation of QSAR Models
By multiple linear regression (MLR) analysis the correlation between physicochemical descriptors and the biological activity was obtained. The total variance in the training set was confirmed by correlation coefficient (r^2), internal predictive ability was confirmed by cross-validated correlation coefficient (q^2), standard deviation for both r^2 (r^2_{se}) and q^2 (q^2_{se}), statistical significance of model was checked by F-test value and external predictive ability was confirmed by predicted correlation coefficient r^2_{pred} and standard deviation r^2_{predse} for the test set compounds. The best models were selected on the basis of higher q^2, lower standard deviation (se), higher F-test values, higher r^2_{pred} and lower r^2_{predse} for the test set compounds.

All the 15 compounds were initially taken for the study. MLR analysis was carried out to find out the factors responsible for variation in the biological activity. It is an attempt to maximize the fit of data to the regression equation by minimizing the squared deviation (standard deviation) from the regression equation for the biological activity and maximizing the variance (r^2) by adjusting each of the available parameter up or down. Sphere exclusion algorithm was used for creating training and test set from the data. The 15 compounds were divided into training set of 10 compounds (~70%) and test set of 5 compounds (~30%).

This model was generated in a stepwise fashion (stepwise multiple regression). That is successive regression equation were derived in which parameters are added, removed or replaced until q^2 and se values are optimized. The magnitude of the coefficients derived in this manner indicates the relative contribution of the associated parameter to the biological activity.

RESULTS AND DISCUSSION

3.1. Characterization Studies
2-(4'-methylbiphenyl-2-yl)-5-aryl-1,3,4-oxadiazole compounds **VMSB 1-15** was synthesized by conventional and microwave assisted synthetic methods by reacting 4'-methyl-[1,1'-biphenyl]-2-carbohydrazide (**2**) with different aryl acids in presence of $POCl_3$ or H_2SO_4. Preparation of these derivatives was faster by microwave methods. Yields of final compounds were in the range of 49-65% after recrystallization from ethanol-water. Structure confirmation of synthesized compounds was done by IR, ^{1}H-NMR, mass and elemental analysis.

Appearance of –NH stretching at 3346 cm^{-1} in the IR spectrum and appearance of peak at δ 2.31, 5.8, 7.11-7.44 ppm in the ^{1}H-NMR spectrum and comparison of the melting points confirmed the structure of compound **2**. IR spectrum of final compounds **VMSB 1-15** showed disappearance of –NH stretching and show prominent IR bands of aromatic skeleton near 3019 cm^{-1} and a sharp peak around 1650-1700 cm^{-1} for the –C=N group. ^{1}H-NMR of **VMSB 1-15** displayed a multiplet at δ 7.11-8.15 for aromatic protons. A singlet was observed at δ 2.34 corresponding to methyl (-CH$_3$) protons. Also, Molecular ion peak M$^+$ of **VMSB 4** and **VMSB 12** at 326.21 and 326.11 respectively, **VMSB 9** at 302.1 and **VMSB 13** at 346 were observed which confirms the structure of synthesized compounds.

3.1.1 4'-methyl-[1,1'-biphenyl]-2-carbohydrazide (2):
Yield: 90-94%; m.p.: 158-160^{0}C; Molecular formula: $C_{14}H_{14}N_2O$ (226); % Elemental Analysis: Calcd. C, 74.31; H, 6.24; N, 12.38; O, 7.07. Found C, 74.42; H, 6.12; N, 12.46; O, 7.16; IR ν$_{max}$ (cm^{-1}) (KBr): 3346, 3021, 1644, 1212, 1102. ^{1}H-NMR (δ ppm; CDCl$_3$): 7.11-7.44 (m, 8H, Ar-CH), 5.8-6.0 (s, 3H, NH/NH$_2$), 2.31 (s, 3H, -CH$_3$).

3.1.2 2-(1H-benzo[d]imidazol-5-yl)-5-(4'-methyl-[1,1'-biphenyl]-2-yl)-1,3,4-oxadiazole (VMSB 1):
Molecular formula: $C_{22}H_{16}N_4O$ (352.39); m.p.: 110-112^{0}C; %Elemental Analysis : Calcd. C, 74.98; H, 4.58; N, 15.90; O, 4.54. Found C, 74.85; H, 4.67; N, 15.79; O, 4.63; IR ν$_{max}$ (cm^{-1})(KBr): 3300 (-NH), 3058 (Ar-CH), 2921 (-CH), 1607 (-C=N), 1292 (-C-N) 1226 (Ar C-O), 739 (-NH wag.); ^{1}H-NMR (δ ppm; CDCl$_3$): 7.22-7.63 (m, 12H, Ar-CH), 4.75 (s, 1H, -NH), 2.37 (s, 3H, -CH$_3$).

_____

3.1.3 2-(4'-methyl-[1,1'-biphenyl]-2-yl)-5-phenyl-1,3,4-oxadiazole (VMSB 2):

Molecular formula: $C_{21}H_{16}N_2O$ (312.36); m.p.: 134-126^{0}C; %Elemental Analysis: Calcd. C, 80.75; H, 5.16; N, 8.97; O, 5.12. Found C, 80.62; H, 5.28; N, 8.86; O, 5.23. IR v_{max} (cm^{-1})(KBr): 3054 (Ar-CH), 2920 (-CH), 1708 (-C=N), 1292 (Ar C-O); ^{1}H-NMR (δ ppm; CDCl$_3$): 7.17-8.67 (m, 12H, Ar-CH), 2.38 (s, 3H, -CH$_3$);

3.1.4 2-(4-bromophenyl)-5-(4'-methyl-[1,1'-biphenyl]-2-yl)-1,3,4-oxadiazole (VMSB 3):

Molecular formula: $C_{21}H_{15}BrN_2O$ (391.26); m.p.: 120-122^{0}C; % Elemental Analysis: Calcd. C, 64.46; H, 3.86; Br, 20.42; N, 7.16; O, 4.09. Found C, 64.35; H, 3.79; Br, 20.31; N, 7.25; O, 4.17; IR v_{max} (cm^{-1})(KBr): 3055 (Ar-CH), 2923 (-CH), 1710 (-C=N), 1067 (Ar C-O), 588 (-C-Br); ^{1}H-NMR (δ ppm; CDCl$_3$): 7.62-8.75 (m, 12H, Ar-CH), 2.38 (s, 3H, -CH$_3$).

3.1.5 2-(4'-methyl-[1,1'-biphenyl]-2-yl)-5-(p-tolyl)-1,3,4-oxadiazole (VMSB 4):

Molecular formula: $C_{22}H_{18}N_2O$ (326.39); m.p.: 116-118^{0}C; % Elemental Analysis: Calcd. C, 80.96; H, 5.56; N, 8.58; O, 4.90. Found C, 80.83; H, 5.63; N, 8.49; O, 4.83; IR v_{max} (cm^{-1})(KBr): 3057 (Ar-CH), 2922 (-CH), 1708 (-C=N), 1179 (Ar C-O); ^{1}H-NMR (δ ppm; CDCl$_3$): 6.59-8.11 (m, 12H, Ar-CH), 2.43 (s, 3H, C$_4$-CH$_3$), 2.33 (s, 3H, C$_2$-CH$_3$); MS: m/z (rel. Int. %): 326 (M$^+$); 312 [(M-14)$^+$]; 298 [(M-28)$^+$]

3.1.6 2-(4'-methyl-[1,1'-biphenyl]-2-yl)-5-(pyridin-2-yl)-1,3,4-oxadiazole (VMSB 5):

Molecular formula: $C_{20}H_{15}N_3O$ (313.35); m.p.: 138-140^{0}C; %Elemental Analysis: Calcd. C, 76.66; H, 4.82; N, 13.41; O, 5.11. Found C, 76.73; H, 4.87; N, 13.34; O, 5.19; IR v_{max} (cm^{-1})(KBr): 3058 (Ar-CH), 2921 (-CH), 1702 (-C=N), 1180 (Ar C-O); ^{1}H-NMR (δ ppm; CDCl$_3$): 7.21-8.75 (m, 12H, Ar-CH), 2.37 (s, 3H, -CH$_3$).

3.1.7 2-(4'-methyl-[1,1'-biphenyl]-2-yl)-5-(o-tolyl)-1,3,4-oxadiazole (VMSB 6):

Molecular formula: $C_{22}H_{18}N_2O$ (326.39); m.p.: 130-132^{0}C; % Elemental Analysis: Calcd. C, 80.96; H, 5.56; N, 8.58; O, 4.90. Found C, 80.85; H, 5.67; N, 8.45; O, 4.79; IR v_{max} (cm^{-1})(KBr): 3049 (Ar-CH), 2946 (-CH), 1725 (-C=N), 1085 (Ar C-O); ^{1}H-NMR (δ ppm; CDCl$_3$): 6.97-8.7 (m, 12H, Ar-CH), 2.44 (s, 3H, C$_4$-CH$_3$), 2.36 (s, 3H, C$_2$-CH$_3$).

3.1.8 2-(4'-methyl-[1,1'-biphenyl]-2-yl)-5-(pyridin-4-yl)-1,3,4-oxadiazole (VMSB 7):

Molecular formula: $C_{20}H_{15}N_3O$ (313.35); m.p.: 121-123^{0}C; %Elemental Analysis: Calcd. C, 76.66; H, 4.82; N, 13.41; O, 5.11. Found C, 76.77; H, 4.69; N, 13.54; O, 5.03; IR v_{max} (cm^{-1})(KBr): 3019 (Ar-CH), 2923 (-CH), 1699 (-C=N), 1135 (Ar C-O); ^{1}H-NMR (δ ppm; CDCl$_3$): 7.19-8.76 (m, 12H, Ar-CH), 2.39 (s, 3H, -CH$_3$).

3.1.9 2-(3-chlorophenyl)-5-(4'-methyl-[1,1'-biphenyl]-2-yl)-1,3,4-oxadiazole (VMSB 8):

Molecular formula: $C_{21}H_{15}ClN_2O$ (346.81); m.p.: 102-104^{0}C; % Elemental Analysis: Calcd. C, 72.73; H, 4.36; Cl, 10.22; N, 8.08; O, 4.61. Found C, 72.63; H, 4.42; Cl, 10.15; N, 8.17; O, 4.74; IR v_{max} (cm^{-1})(KBr): 3054 (Ar-CH), 2929 (-CH), 1597 (-C=N), 1089 (Ar C-O), 738 (-C-Cl); ^{1}H-NMR (δ ppm; CDCl$_3$): 7.29-8.23 (m, 12H, Ar-CH), 2.34 (s, 3H, -CH$_3$).

3.1.10 2-(furan-2-yl)-5-(4'-methyl-[1,1'-biphenyl]-2-yl)-1,3,4-oxadiazole (VMSB 9):

Molecular formula: $C_{19}H_{14}N_2O_2$ (302.33); m.p.: 49-51^{0}C; %Elemental Analysis: Calcd. C, 75.48; H, 4.67; N, 9.27; O, 10.58. Found C, 75.37; H, 4.79; N, 9.22; O, 10.67; IR v_{max} (cm^{-1})(KBr): 3027 (Ar-CH), 2919 (-CH), 1709 (-C=N), 1180 (Ar C-O); ^{1}H-NMR (δ ppm; CDCl$_3$): 6.37-7.61 (m, 12H, Ar-CH), 2.36 (s, 3H, -CH$_3$); MS: m/z (rel. Int. %): 302([M]$^+$,18); 301([M-1]$^+$, 100); 279.1 ([M-28]$^+$, 9)

3.1.11 2-(4-methoxyphenyl)-5-(4'-methyl-[1,1'-biphenyl]-2-yl)-1,3,4-oxadiazole (VMSB 10):

Molecular formula: $C_{22}H_{18}N_2O_2$ (342.39); m.p.: 86-89^{0}C; %Elemental Analysis: Calcd. C, 77.17; H, 5.30; N, 8.18; O, 9.35. Found C, 77.24; H, 5.19; N, 8.26; O, 9.27; IR v_{max} (cm^{-1})(KBr): 3038 (Ar-CH), 2923 (-CH), 1712 (-C=N), 1172 (C-O); ^{1}H-NMR (δ ppm; CDCl$_3$): 6.94-8.61 (m, 12H, Ar-CH), 3.85 (s, 3H, -OCH$_3$), 2.44 (s, 3H, -CH$_3$).

3.1.12 2-(4-fluorophenyl)-5-(4'-methyl-[1,1'-biphenyl]-2-yl)-1,3,4-oxadiazole (VMSB 11):

Molecular formula: $C_{21}H_{15}FN_2O$ (330.36); m.p.: 88-90^{0}C; %Elemental Analysis: Calcd. C, 76.35; H, 4.58; F, 5.75; N, 8.48; O, 4.84. Found C, 76.48; H, 4.49; F, 5.83; N, 8.37; O, 4.93; IR v_{max} (cm^{-1})(KBr): 3078 (Ar-CH), 2936 (-CH), 1714 (-C=N), 1198 (Ar C-O), 1028 (-C-F); ^{1}H-NMR (δ ppm; CDCl$_3$): 7.11-8.62 (m, 12H, Ar-CH), 2.39 (s, 3H, -CH$_3$).

3.1.13 2-(4'-methyl-[1,1'-biphenyl]-2-yl)-5-(m-tolyl)-1,3,4-oxadiazole (VMSB 12):

Molecular formula: $C_{22}H_{18}N_2O$ (326.39); m.p.: 113-115^{0}C; % Elemental Analysis: Calcd. C, 80.96; H, 5.56; N, 8.58; O, 4.90. Found C, 80.87; H, 5.45; N, 8.67; O, 4.96; IR v_{max} (cm^{-1})(KBr): 3064 (Ar-CH), 2922 (-CH), 1684 (-

_____

C=N), 1039 (Ar C-O); ^{1}H-NMR (δ ppm; CDCl$_3$): 7.19-8.78 (m, 12H, Ar-CH), 2.48 (s, 3H, C$_4$-CH$_3$), 2.31 (s, 3H, C$_2$-CH$_3$); MS: m/z (rel. Int. %): 326 (M$^+$); 312 [(M-14)$^+$]; 298 [(M-28)$^+$].

3.1.14 2-(4-chlorophenyl)-5-(4'-methyl-[1,1'-biphenyl]-2-yl)-1,3,4-oxadiazole (VMSB 13):
Molecular formula: C$_{21}$H$_{15}$ClN$_2$O (346.81); m.p.: 113-115^{0}C; % Elemental Analysis: Calcd. C, 72.73; H, 4.36; Cl, 10.22; N, 8.08; O, 4.61. Found C, 72.85; H, 4.31; Cl, 10.10; N, 8.21; O, 4.56; IR ν_{max} (cm^{-1})(KBr): 3049 (Ar-CH), 2997 (-CH), 1625 (-C=N), 1088 (Ar C-O), 702 (-C-Cl); ^{1}H-NMR (δ ppm; CDCl$_3$): 7.27-8.13 (m, 12H, Ar-CH), 2.37 (s, 3H, -CH$_3$); MS: m/z (rel. Int. %): 346 (M$^+$, 100); 348 [(M+2)$^+$, 95).

3.1.15 2-(2-bromophenyl)-5-(4'-methyl-[1,1'-biphenyl]-2-yl)-1,3,4-oxadiazole (VMSB 14):
Molecular formula: C$_{21}$H$_{15}$BrN$_2$O (391.26); m.p.: 92-94^{0}C; %Elemental Analysis: Calcd. C, 64.46; H, 3.86; Br, 20.42; N, 7.16; O, 4.09. Found C, 64.57; H, 3.97; Br, 20.53; N, 7.07; O, 4.14; IR ν_{max} (cm^{-1})(KBr): 3021 (Ar-CH), 2944 (-CH), 1687 (-C=N), 1072 (Ar C-O), 685 (-C-Br); ^{1}H-NMR (δ ppm; CDCl$_3$): 7.46-8.86 (m, 12H, Ar-CH), 2.55 (s, 3H, -CH$_3$).

3.1.16 2-(2H-indol-3-yl)-5-(4'-methyl-[1,1'-biphenyl]-2-yl)-1,3,4-oxadiazole (VMSB 15):
Molecular formula: C$_{23}$H$_{17}$N$_3$O (351.40); m.p.: 94-96^{0}C; %Elemental Analysis: Calcd. C, 78.61; H, 4.88; N, 11.96; O, 4.55. Found C, 78.49; H, 4.97; N, 11.87; O, 4.69; IR ν_{max} (cm^{-1})(KBr): 3146 (Ar-CH), 2926 (-CH), 1687 (-C=N), 1240 (Ar C-O); ^{1}H-NMR (δ ppm; CDCl$_3$): 6.37-7.61 (m, 12H, Ar-CH), 2.54 (s, 3H, -CH$_2$), 2.36 (s, 3H, -CH$_3$).

3.2 Acute oral toxicity
The acute toxicity of **VMSB 11** in mice was found to be greater than 2000 mg/kg. No lethality or any toxic reactions were found up to the anti-inflammatory dose range. All the compounds were having LD$_{50}$ greater than 2000 mg/kg.

3.3 Analgesic activity
Comparison of analgesic activity carried out by using the acetic acid induced writhing model is given in Table 1 and Fig. 2. Writhing test is based on the principle that tissue injury increases the sensitivity to pain and this sensitivity is susceptible to modification by analgesics [21]. Compounds **VMSB 2, VMSB 4, VMSB 6, VMSB 11**, and **VMSB 12** were active compounds in the present series. These compounds exhibited peripheral analgesic activity like most of the NSAIDs.

Table 1 Effect of VMSB 1-15 series on writhing induced by acetic acid in mice

Group	No. of Writhings ±SEM	% inhibition
Acetic Acid Control	60 ± 1.7	-
VMSB1	49 ± 2.1	18.33**
VMSB2	30 ± 1.5	50***
VMSB3	51 ± 1.6	15*
VMSB4	33 ± 1.2	45***
VMSB5	47 ± 1.7	21.67***
VMSB6	35 ± 1.6	41.67***
VMSB7	49 ± 2.7	18.33**
VMSB8	42 ± 2.4	30***
VMSB9	47 ± 2.6	21.67***
VMSB10	50 ± 1.9	16.67**
VMSB11	29 ± 1.3	51.67***
VMSB12	31 ± 1.1	48.33***
VMSB13	52 ± 1.1	13.33*
VMSB14	45 ± 2.1	25***
VMSB15	51 ± 1.6	15*
Diclofenac	25 ± 2.3	58.33***

*Values are mean ± SEM., n=6 in each group; Statistical analysis by One-way ANOVA followed by post hoc Dunnett's test using Graphpad Instat software; P value *<0.05; **<0.01; ***<0.001 compared to vehicle treated group.*
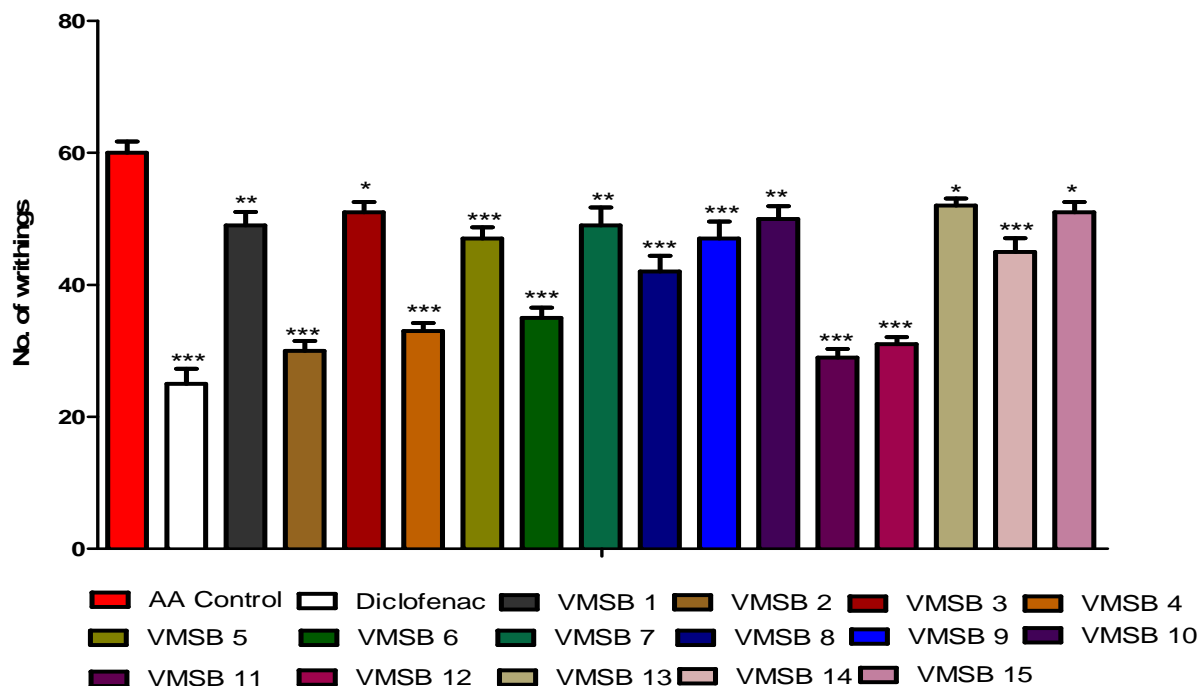
_____

Figure 2 Analgesic activity of VMSB 1-15 compared with standard drug determined by acetic acid induced writhing in mice

3.4 Anti-inflammatory activity

Comparison of the anti-inflammatory activity was determined using the carrageenan-induced rat paw edema assay and results are given in Table 2. The pharmacological experiments of this study showed that among the tested compounds **VMSB 2, VMSB 4, VMSB 6, VMSB 8, VMSB 11, VMSB 12** and **VMSB 14** exhibited promising anti-inflammatory activities as compared to standard NSAIDs. Diclofenac sodium was used as a standard drug for comparing the anti-inflammatory activity (Fig. 3).

Carrageenan induced paw edema is biphasic, of which the first phase is mediated by the release of histamine and 5-hydroxytryptamine followed by kinin release and then prostaglandin in the later phase [37]. It has been reported that the second phase (3 hour) of edema is sensitive to most clinically effective anti-inflammatory agents. Anti-inflammatory effects of these series in third hour of edema suggest involvement of inhibition of prostaglandin. Compound **VMSB 11** has statistically significant activity in the series. Compounds **VMSB 2, VMSB 4, VMSB 6, VMSB 8, VMSB 12** and **VMSB 14** also have prominent activity in the series.

_____

Table 2 Effect of VMSB 1-15 series on carrageenan induced rat hind paw edema

Group	Difference in paw volume at hrs (Mean ± SEM) (% Inhibition)		
	1 h	**3 h**	**5 h**
Carrageenan Control	1.35 ± 0.05	1.59 ± 0.03	1.98 ± 0.03
Diclofenac	1.23 ± 0.03 (7.31)	1.12 ± 0.02*** (29.71)	0.91 ± 0.03*** (54.33)
VMSB 1	1.25 ± 0.02 (7.06)	1.29 ± 0.03*** (19.25)	1.27 ± 0.03*** (35.91)
VMSB 2	1.25 ± 0.03 (7.43)	1.17 ± 0.03*** (26.78)	0.97 ± 0.03*** (50.88)
VMSB 3	1.28 ± 0.05 (5.08)	1.46 ± 0.04* (8.68)	1.66 ± 0.04*** (16.32)
VMSB 4	1.23 ± 0.04 (8.43)	1.21 ± 0.04*** (24.06)	1.05 ± 0.05*** (47.10)
VMSB 5	1.24 ± 0.03 (7.56)	1.26 ± 0.03*** (20.92)	1.17 ± 0.03*** (40.96)
VMSB 6	1.25 ± 0.02 (7.15)	1.22 ± 0.02*** (23.74)	1.06 ± 0.03*** (46.51)
VMSB 7	1.25 ± 0.02 (6.94)	1.32 ± 0.02*** (17.36)	1.41 ± 0.04*** (28.68)
VMSB 8	1.23 ± 0.02 (8.55)	1.22 ± 0.03*** (23.33)	1.06 ± 0.02*** (46.34)
VMSB 9	1.24 ± 0.04 (7.68)	1.26 ± 0.03*** (21.03)	1.24 ± 0.03*** (37.59)
VMSB 10	1.26 ± 0.04 (6.69)	1.35 ± 0.04*** (15.27)	1.48 ± 0.03*** (25.23)
VMSB 11	1.25 ± 0.04 (7.06)	1.17 ± 0.06*** (26.88)	0.96 ± 0.05*** (51.47)
VMSB 12	1.25 ± 0.03 (7.06)	1.20 ± 0.04*** (24.99)	1.00 ± 0.03*** (49.79)
VMSB 13	1.26 ± 0.04 (6.44)	1.44 ± 0.04** (9.62)	1.59 ± 0.04*** (19.85)
VMSB 14	1.24 ± 0.01 (7.81)	1.24±0.01*** (22.28)	1.11±0.02*** (44.15)
VMSB 15	1.27 ± 0.03 (5.95)	1.45 ± 0.04** (9.10)	1.64 ± 0.05*** (17.49)

Values are mean ± SEM., n=6 in each group; Statistical analysis by Two-way ANOVA followed by post hoc Dunnett's test using Graphpad Instat software; P value *<0.05; **<0.01; ***<0.001 compared to vehicle (gum acacia, 10 ml/kg) treated group. The figures in parentheses indicate the percent inhibition.
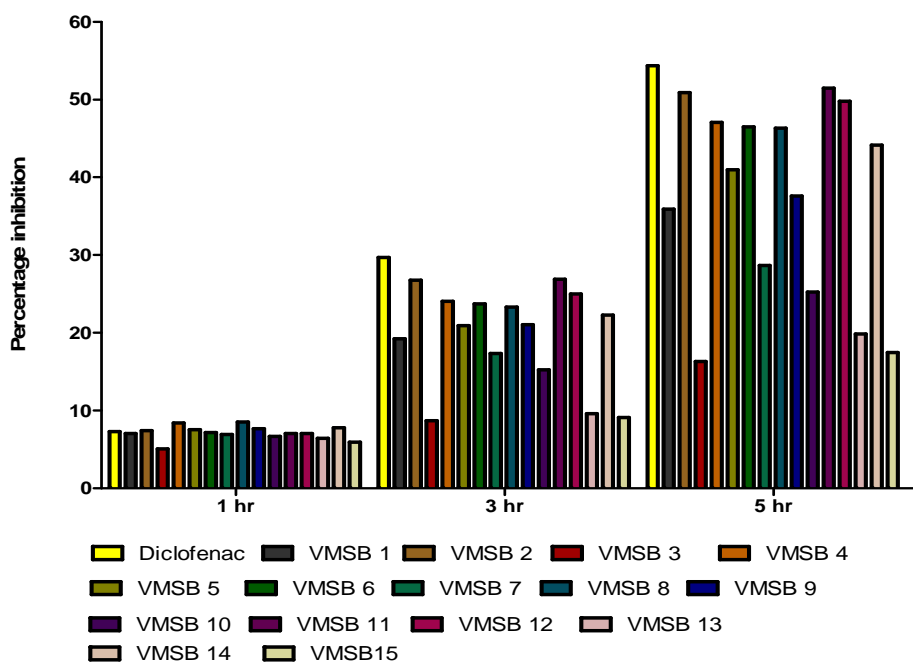
Figure 3 Anti-inflammatory activity of VMSB 1-15 compared with standard drug determined by carrageenan induced rat hind paw edema

_____

3.5 Cotton pellet induced granuloma in rats

Cotton pellet induced granuloma formation is considered to be reliable experimental model for evaluation of effects of macrophage dysfunction and granuloma formation, central players in the formation, maintenance and progression of granulomas in various disease states [38-39]. **VMSB 2**, **VMSB 11,** and **VMSB 12** (10 mg/kg) significantly ($p<0.001$) inhibited the granuloma formation with 40.74%, 44.44% and 39.51% inhibition respectively, when compared to vehicle control group (Fig. 4). Diclofenac (10mg/kg) significantly ($p<0.001$) inhibited the granuloma formation with maximum inhibition of 62.96 % (Table 3).

Table 3 Effect of VMSB compounds on dry weight of granuloma in cotton pellet-induced granuloma in rats

Group	Increased dry weight of granuloma (mg)	(% Inhibition)
Vehicle control	81±3.8	-
Diclofenac	30±1.3***	62.96
VMSB 2	48±2.2***	40.74
VMSB 11	45±1.9***	44.44
VMSB 12	49±2.1***	39.51

*Values are expressed as mean ± SEM for six animals and analysed by One way ANOVA followed by Dunnett's test, ***p< 0.001 when compared to vehicle control.*
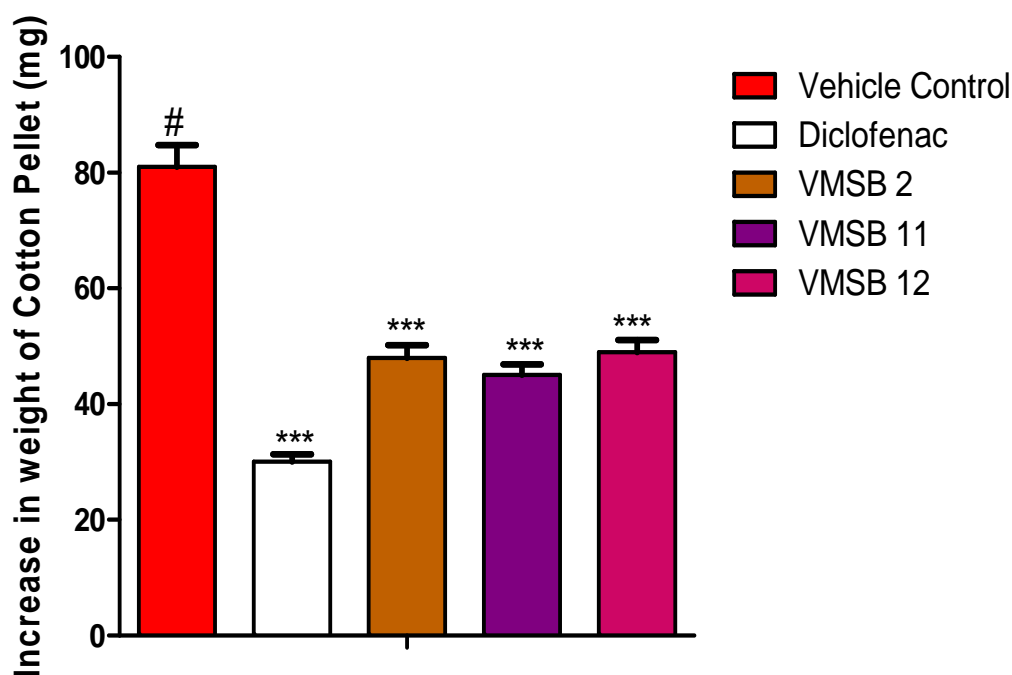
Figure 4 Anti-inflammatory activity of selective VMSB compounds compared with standard drug determined using the cotton pellet induced granuloma model

3.6 Acute ulcerogenicity studies

The active compounds **VMSB 2, VMSB 11** and **VMSB 12** which possessed promising analgesic activity and anti-inflammatory activity were further screened for ulcerogenic activity of stomach. Compounds **VMSB 2, VMSB 11** and **VMSB 12** showed less signs of gastric ulceration compared to standard drug. The ulcer index is shown in Table 4. A less incidence of gastric erosion was observed for the highest active compound **VMSB 11**.

_____

Diclofenac   VMSB 2
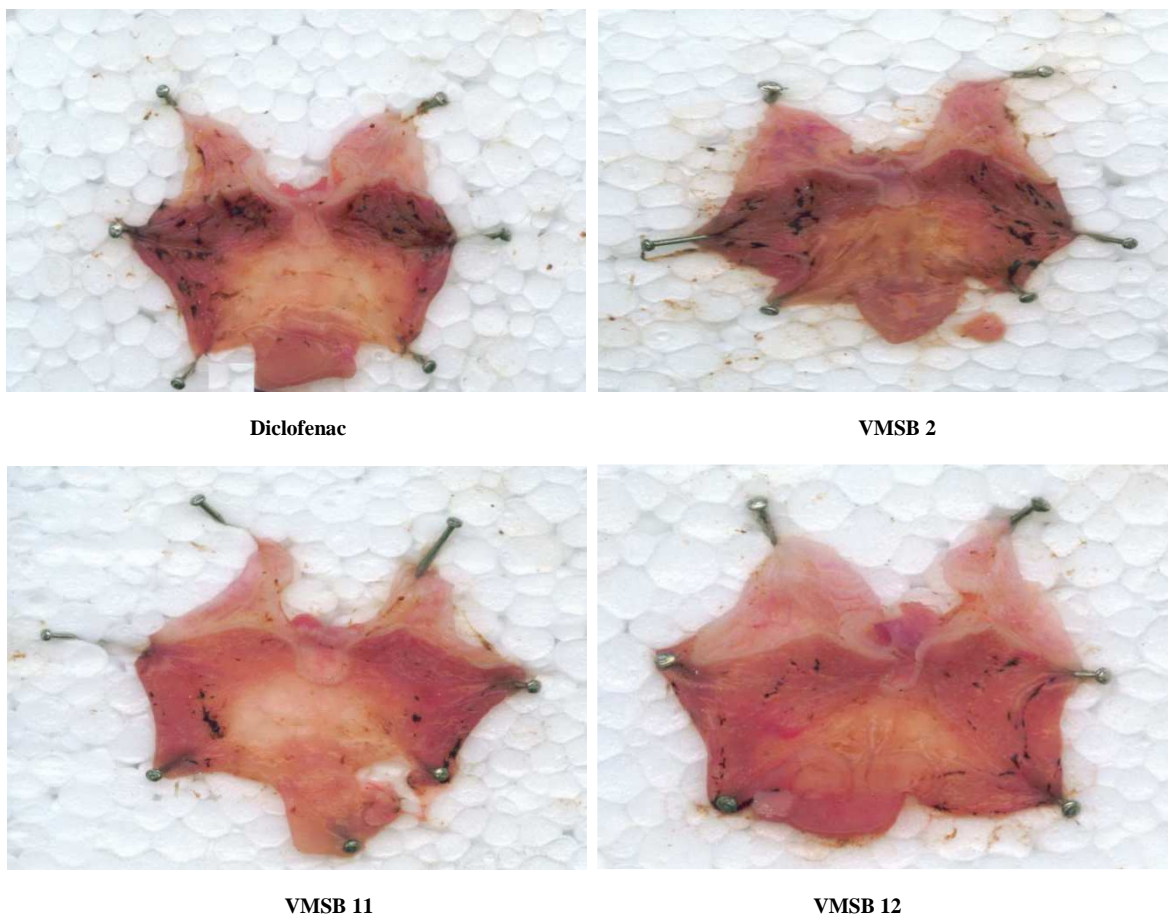
VMSB 11   VMSB 12

Figure 5 Photographic representation of ulcer in rat stomach. The dark coloured marks found in rat stomach indicates ulcer patch

Table 4 Ulcer index for the most active compounds

Compound	Ulcer Index
VMSB 2	1.47
VMSB 11	0.79
VMSB 12	1.03
Diclofenac	1.72

3.7 Histopathology study

The stomach specimen of diclofenac treated rats showed complete disruption of protective mucosal layer. Histopathological analysis showed characteristic features of ulceration in diclofenac treated group of animals (Fig. 6b). The tissue of diclofenac treated rats showed that some epithelial cells in the ulcer margin had proliferated and migrated over and into the ulcer crater, which was strongly infiltrated by inflammatory cells, indicating complete disruption of gastric epithelial layer. Scanning of stomach specimens using electron microscope revealed that rats treated with **VMSB 11** specimen (Fig. 6c) showed less gastric mucosal injury compared with diclofenac treated group, while disruption of gastric epithelial layer was observed in **VMSB 2** and **VMSB 12** treated rat specimen as observed in Fig. 6d and Fig. 6e respectively but less than diclofenac. Finally, histopathology study of stomach in cotton pellet induced granuloma in rats showed sign of gastric ulcerations and damage of mucosal membrane due to diclofenac treated rat specimen. **VMSB 2, VMSB 11** and **VMSB 12** showed less damage to mucosal layer of GI lining.
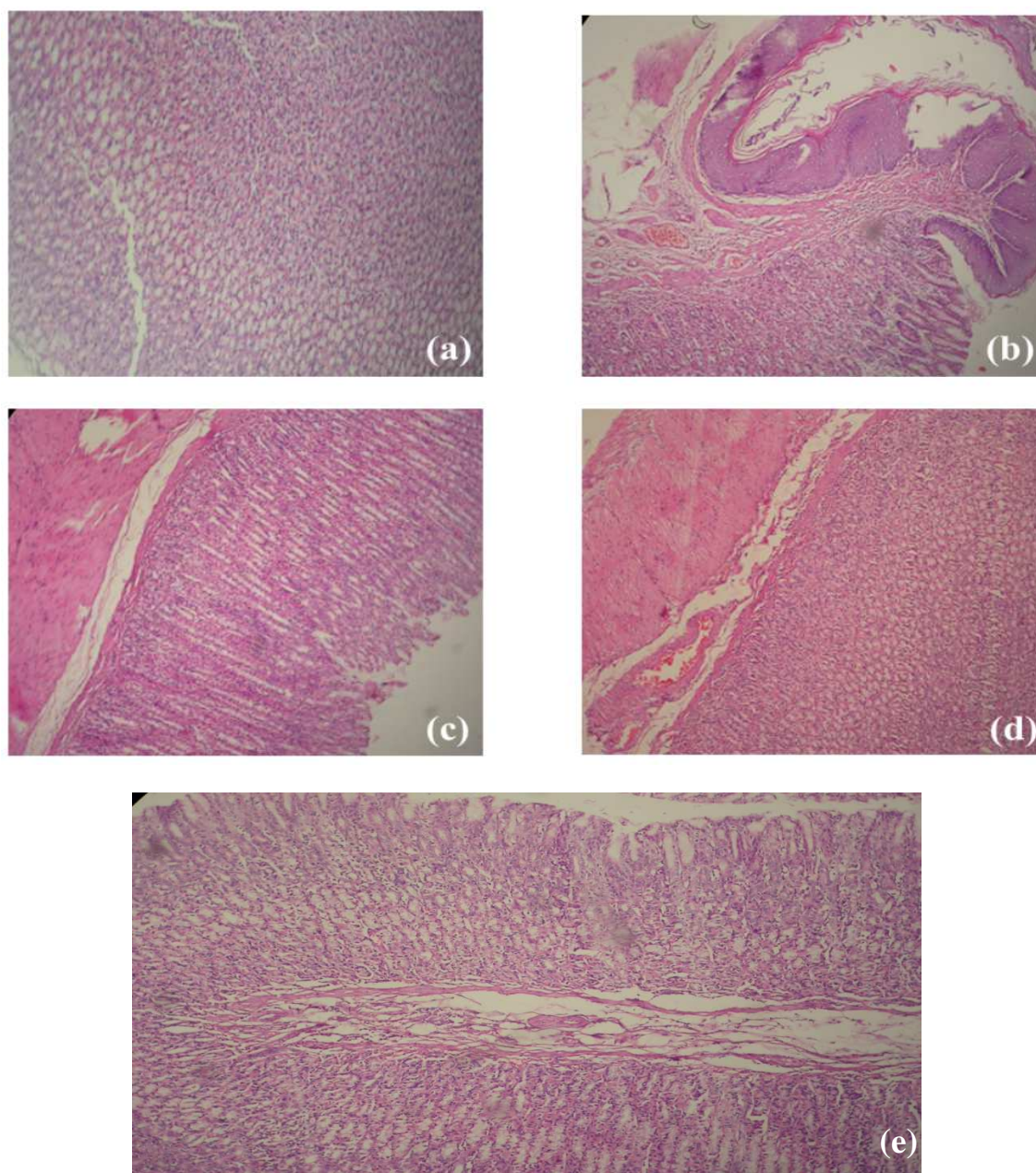
Figure 6 Histopathology of stomach of cotton pellet induced granuloma in rats. As illustrated in figure specimen: (a) showed intact mucous membrane in control treated rat showing granular tissues composed of macrophages, fibroblasts and endothelial cells forming microvessels. (b) Congestion of mucosal blood vessels was observed in diclofenac treated group. (c) Less gastric damage was observed to mucosa of rat treated with test compound, VMSB 11 specimen. (d) Disruption of gastric epithelial layer was observed for VMSB 2 specimen but less than diclofenac. (e) Disruption of gastric epithelial layer was observed for VMSB 12 specimen but less than diclofenac. The observations of test groups were compared to that of the control

3.8 Docking studies

Docking was carried out to study the binding mode of the compound **VMSB 11** with the active site of COX-2 to obtain selective information for further structure optimization. The structure based docking studies were performed using Glide Extra-precision (XP) docking module.

The bulky biphenyl forms the π-π stacking with Arg120 in the hydrophobic pocket. Also, 4-fluro phenyl fits into the hydrophobic cavity induced by amino acids Tyr355 and Trp387 and shows the π-π stacking with these amino acids.

The docking results of **VMSB 11** with COX-2 are given in Fig. 7 and Fig. 8. The Glide docking score of **VMSB 11** was found to be −10.091. From the docking study it is observed that this ligand binds to sub pockets in the active site: the hydrophobic clamp formed by the residues Arg120, Tyr355, Tyr385 and Trp387 which play an important role for COX-2 inhibition. Docking score of all the compounds is reported in Table 6.

168
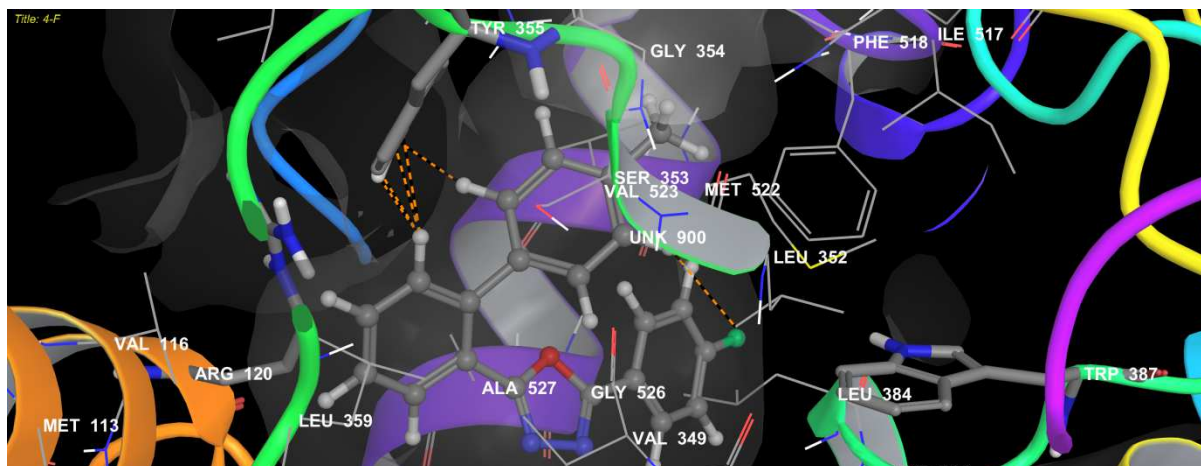
Figure 7 Docking of compound VMSB 11 in the active site of COX-2
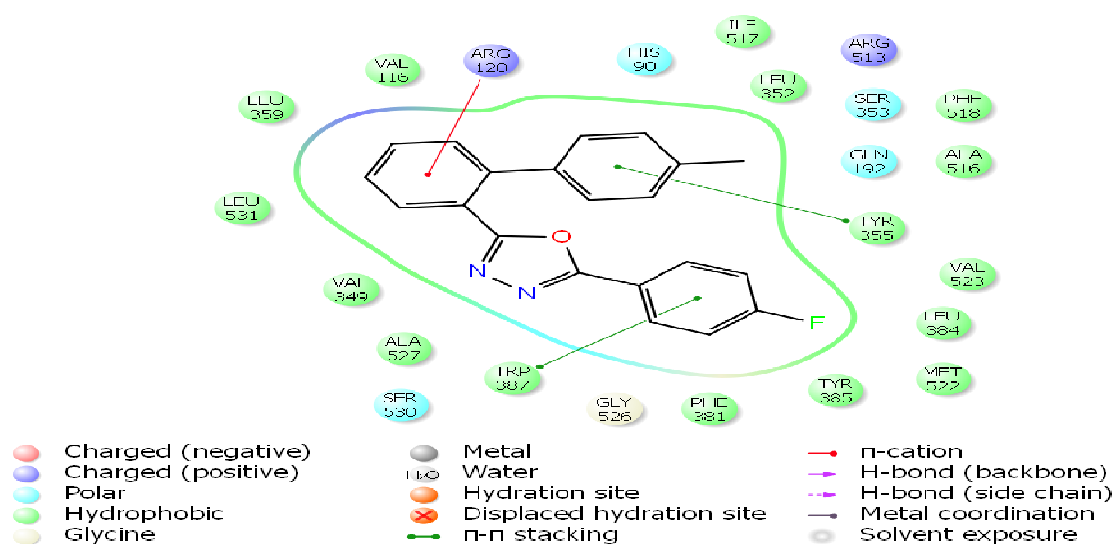
Figure 8 2D view of the binding interaction of the compound VMSB 11 with the active site of COX-2

3.9 ADME studies

All the forty-four pharmaceutically relevant descriptors available in QikProp were calculated for the synthesized compounds. The important descriptors like QPlogPo/w, QPlogS, QPlogHERG, QPPCaco, QPlogBB, QPlogKhsa and % human oral absorption are given in Table 5. For all the compounds, the partition coefficient (QPlogPo/w) and water solubility (QPlogS) critical for estimating the absorption and distribution of drugs within the body ranged between 5.808 to 4.250 and -6.472 to -5.262 respectively. The blood brain barrier partition coefficient QPlogBB ranged from -0.584 to 0.201. QPlogHERG varied from -6.844 to -5.977. QPPCaco and QPlogKhsa varied from 4098.143 to 876.451 and 1.137 to 0.521 respectively. Further, the percentage human oral absorption was found to be 100% for all the compounds. The pharmacokinetic parameters for the entire 15 synthesized compound were found to be within the acceptable range defined for human use revealing their potential as possible drug-like compounds.

_____

Table 5 ADME properties of the synthesized compounds

Compound Code	QPlogPo/w	QPlogS	QPlogHERG	QPPCaco	QPlogBB	QPlogKhsa	% Human Oral absorption
VMSB 1	4.25	-5.568	-5.977	876.451	-0.584	0.762	100
VMSB 2	5.115	-6.185	-6.844	4066.934	0.035	0.961	100
VMSB 3	5.808	-6.206	-6.799	4069.014	0.213	1.117	100
VMSB 4	5.539	-6.427	-6.771	4071.395	0.023	1.137	100
VMSB 5	4.591	-5.731	-6.753	2619.989	-0.169	0.657	100
VMSB 6	5.448	-6.472	-6.439	3961.981	0.032	1.078	100
VMSB 7	4.274	-5.378	-6.623	2207.174	-0.24	0.521	100
VMSB 8	5.549	-6.078	-6.765	4073.581	0.202	1.09	100
VMSB 9	4.515	-5.262	-6.367	3790.692	0.02	0.607	100
VMSB 10	5.393	-6.464	-6.754	4070.439	-0.036	0.938	100
VMSB 11	5.335	-6.312	-6.729	4070.215	0.147	1.01	100
VMSB 12	5.538	-6.422	-6.767	4075.69	0.024	1.136	100
VMSB 13	5.552	-6.085	-6.77	4069.536	0.201	1.091	100
VMSB 14	5.586	-6.433	-6.41	4098.143	0.185	1.065	100
VMSB 15	5.048	-6.36	-6.668	2506.095	-0.197	0.859	100

QPlogPo/w: Predicted octanol/water partition coefficient (-2.0 to 6.5)
QPlogS: Predicted aqueous solubility in mol dm^{-3} (-6.5 to 0.5)
QPlogHERG: Predicted IC_{50} value for blockage of HERG K+ channels (acceptable range: below −6.0)
QPPCaco: Predicted apparent Caco-2 cell (gut-blood barrier model) permeability in nm/sec (< 25 poor; > 500 excellent)
QPlogBB: Predicted brain/blood partition coefficient (-3 to 1.2)
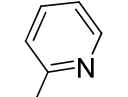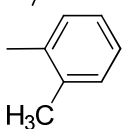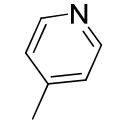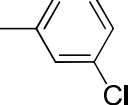*QPlogKhsa: Prediction of binding to human serum albumin (-1.5 to 0.5)*
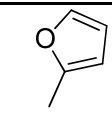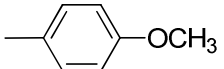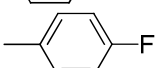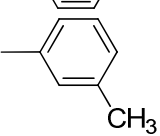*% Human oral absorption: Predicted human oral absorption (< 25 poor; > 80 high)*
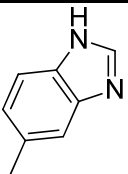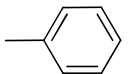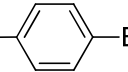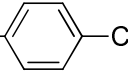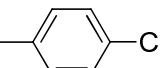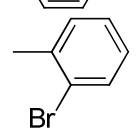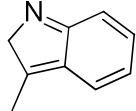
3.10QSAR Studies
3.10.1 Chemical Data
A set of 15 synthesized compounds belonging to biphenyl-2-oxadiazole analogues were taken for QSAR study. The biological activity (BA) was expressed as logarithm of BA value in % Inhibition. (Table 6)

Table 6 Biological activity of the biphenyl-2-oxadiazole analogues

Compound Code	R	%BA	LogBA	Predicted BA	Docking Score
VMSB 1		35.91	1.555	1.511	-8.570
VMSB 2*		50.88	1.706	1.550	-10.053
VMSB 3		16.32	1.2127	1.202	-6.934
VMSB 4*		47.10	1.673	1.567	-9.858
VMSB 5*		40.96	1.612	1.557	-9.152
VMSB 6		46.51	1.667	1.676	-9.845
VMSB 7		28.68	1.457	1.547	-8.528
VMSB 8*		46.34	1.665	1.527	-9.557

_____

VMSB 9*		37.59	1.575	1.630	-9.100
VMSB 10		25.23	1.401	1.441	-7.845
VMSB 11		51.47	1.711	1.551	-10.091
VMSB 12		49.79	1.697	1.598	-9.857
VMSB 13		19.85	1.297	1.421	-7.010
VMSB 14		44.15	1.644	1.713	-9.156
VMSB 15		17.49	1.242	1.218	-7.002

Log BA: Logarithm of biological activity (%BA)
*Test Set Compounds

3.10.2 Multiple Linear Regression analysis

QSAR study was performed for a series of biphenyl-2-oxadiazole analogues. Multiple linear regression (MLR) analysis was performed to find the correlation between physicochemical properties and the biological activity. The best QSAR model obtained is shown in the Table 7.

Table 7 Best QSAR Model

Sr.No.	Equation	n	r^2	q^2	F	r^2_{se}	q^2_{se}	r^2_{Pred}	r^2_{predse}
1.	Log 1/BA = -0.0655 (±0.0128) Radius of gyration+0.1396 (±0.0473)SaasCcount +1.5751	15	0.897	0.672	19.763	0.098	0.125	0.554	0.122

This equation is the best model for the present series of 15 compounds. It shows correlation between Radius of gyration, SaasCcount and biological activity.

The equation explains ~90 % (r^2= 0.897) of the total variance in the training set as well as it has internal (q^2) and external (r^2_{pred}) predictive ability of ~67 % and ~55% respectively. The F test = 19.73 shows the statistical significance of ~62% of the model which means that probability of failure of the model is 1 in 1000.

The data and graph of observed and predicted biological activity is given in Table 6 and Fig. 9 respectively. The radar plot depicts the closeness between the actual and predicted activity of the compounds of training and test set (Fig. 10). Also, the contribution plot of each descriptor is given in Fig. 11.

The plot of observed versus predicted activity shows that the model is able to predict the activity of training set well as well as external test set up to ~55% providing confidence in predictive ability of the model.
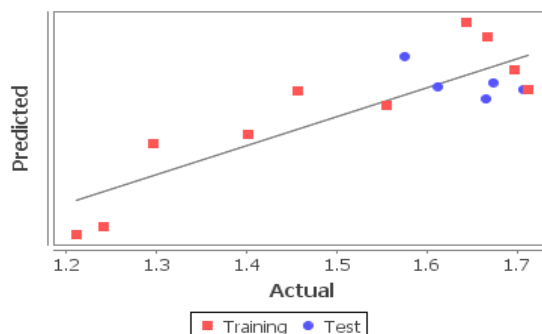
Figure 9 Observed and predicted biological activity of training and test compounds
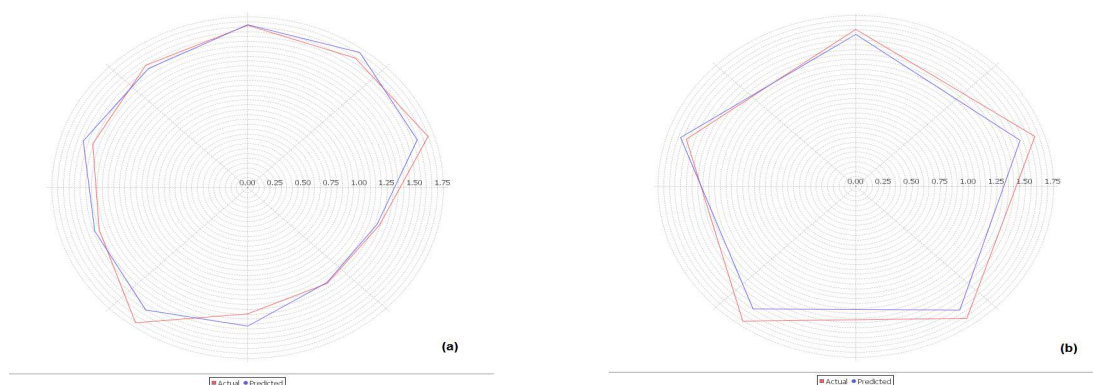
171

_____

Figure 10 Radar plots showing alignment of actual and predicted activities of the compounds of training (a) and test set (b)
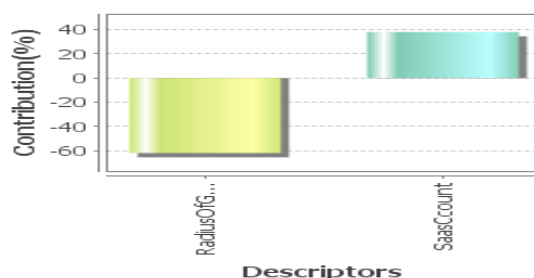

Figure 11 Contribution plot of descriptors

Radius of gyration is a distance based Geometric descriptor with subclass of Distance based Topological descriptor and SaasCcount is an Electrotopological State Indices descriptor with subclass of Atom Type Count Non-hydrogen Indices descriptor.

The developed regression model reveals that the negative correlation of biological activity with descriptor Radius of gyration (61%) (The size descriptor for the distribution of atomic masses in a molecule) indicates that decrease in the size of atomic masses will improve the biological activity. The next most important factor influencing activity variation is SaasCcount (39%) (Total number of carbon connected with one single bond along with two aromatic bonds) and is directly proportional to the activity, shows the role of presence of biphenyl ring to be important for the activity.

CONCLUSION

A novel series of biphenyl analogues was designed by molecular modeling and docking studies. The designed compounds were synthesized by conventional and microwave assisted methods. Structure of synthesized compounds was confirmed by IR, ^{1}H-NMR, mass and elemental analysis and screened for analgesic and anti-inflammatory activity by *in vivo* models. The compound **VMSB 11** was found as the most active. The synthesized compounds **VMSB 2, VMSB 4, VMSB 6, VMSB 8, VMSB 11**, **VMSB 12** and **VMSB 14** exhibited significant analgesic and anti-inflammatory activity compared to standard drug. Furthermore, these compounds showed little ulcerogenic activity compared to diclofenac. The synthesized compounds along with their anti-inflammatory activity were further subjected for docking and QSAR studies. The compound **VMSB 11** shows good binding with COX-2 receptor with docking score of -10.091 and it shows π-π stacking with Arg120, Tyr355 and Trp387 and fits into hydrophobic pocket formed by these amino acids. The developed regression model reveals the importance of presence of biphenyl ring and suggests that decrease in the size of atomic masses will improve the biological activity. A good statistical correlation ($q^2 = 0.672$) with biological activity was obtained. Also, the pharmacokinetic parameters for the entire 15 synthesized compounds were found to be within the acceptable range defined for human use revealing their potential as possible drug-like compounds. Hence these compounds can serve as good leads for further modification and optimization to obtain better compounds.

172

_____

Bharati Vidyapeeth University, Pune and Dr. K. R. Mahadik, Principal, Poona College of Pharmacy, Pune for their encouragement.

REFERENCES

[1] J.R. Vane, *Nature.*, **2005**, 367, 215.
[2] J.M. Dogne, C.T. Supuran, D. Pratico, *J. Med. Chem.*, **2005**, 48, 2251.
[3] S. Bansal, M. Bala, S.K. Suthar, S. Choudhary, S. Bhattacharya, V. Bhardwaj, S. Singla, A. Joseph, *Eur. J. Med. Chem.*, **2014**, 80, 167.
[4] D.V. Dekhane, S.S. Pawar, S. Gupta, M.S. Shingare, C.R. Patil, S.N. Thore, *Bioorg. Med. Chem. Lett.*, **2011**, 21, 6527.
[5] U.A. Shah, N.K. Wagh, H.S. Deokar, S.S. Kadam, V.M. Kulkarni, *Int. J. Pharm. Bio. Sci.*, **2010**, 1, 501.
[6] U.A. Shah, N.K. Wagh, H.S. Deokar, S.S. Kadam, V.M. Kulkarni, *Int. J. Pharm. Bio. Sci.*, **2010**, 1, 512.
[7] V.M. Kulkarni, R.R. Sakhardande, N.K. Wagh, M. Nimbalkar, S.M. Nadkarni, U.S. Patent 8,236,843 B2, August 27, **2012**.
[8] A. Husain, A. Ahmad, M.M. Alam, M. Ajmal, P. Ahuja, *Eur. J. Med. Chem.*, **2009**, 44, 3798.
[9] M.M. Burbuliene, V. Jakubkiene, G. Mekuskiene, E. Udrenaite, R. Smicius, P. Vainilavicius, *Farmaco.*, **2004**, 59, 767.
[10] H. Kumar, S.A. Javed, S.A. Khan, M. Amir, *Eur. J. Med. Chem.*, **2008**, 4, 2688.
[11] V. Jakubkiene, M.M. Burbuliene, G. Mekuskiene, E. Udrenaite, P. Gaidelis, P. Vainilavicius, *Farmaco.*, **2003**, 58, 323.
[12] M. Akhter, A. Husain, B. Azad, M. Ajmal, *Eur. J. Med. Chem.*, **2009**, 44, 2372.
[13] T. Chandra, N. Garg, S. Lata, K.K. Saxena, A. Kumar, *Eur. J. Med. Chem.* **2010**, 45, 1772.
[14] E. Palaska, G. Sahin, P. Kelicen, N.T. Durlu, G. Altinok, *Farmaco.*, **2002**, 47, 101.
[15] B. Jayashankar, K.M. Lokanath Rai, N. Baskaran, H.S. Sathish, *Eur. J. Med. Chem.*, **2009**, 44, 3898.
[16] S.V. Bhandari, K.G. Bothara, M.K. Raut, A.A.Patil, A.P.Sarkate, V.J. Mokale, *Bioorg. Med. Chem.*, 2008, 16, 1822.
[17] M. Amir, H. Kumar, S.A. Javed*, Eur. J. Med. Chem.*, **2008**, 43, 2688.
[18] M. Amir, K. Shikha, *Eur. J. Med. Chem.*, **2004**, 39, 535.
[19] K. Manjunatha, B. Poojary, P.L. Lobo, J. Fernandes, N.S. Kumari, *Eur. J. Med. Chem.*, **2010**, 45, 5225.
[20] Guidance document on acute oral toxicity testing environment directorate, Organisation for Economic Co-operation and Development (OECD), Paris, **2001**, 1.
[21] H.O Collier, L.C. Dinneen, C.A. Johnson, C. Schneider, *Br. J. Pharmacol.* **1968**, 32, 295.
[22] C.A. Winter, E.A. Risley, W.G. Nuss, *Proc. Soc. Exp. Biol. Med.*, **1962**, 111, 544.
[23] W.H. Vogel, B.A. Scholkens, J. Sandow, G. Muller, In: H.G. Vogel (Ed.), Drug discovery and evaluation-pharmacological assays (Springer-Verlag Berlin, Hiedelberg, 2008) 406.
[24] P. D'Arcy, E. Haward, P. Muggleton, S. Townsend, *J. Pharm. Pharmacol.*, **1960**, 12, 659.
[25] M. Grau, J.L. Guasch, A. Montero, *Drug. Res.*, **1991**, 41, 1265.
[26] Glide, version 5.8, Schrödinger LLC, New York, NY, 2012; Software available at http://www.schrodinger.com.
[27] R.G. Kurumbail, A.M. Stevens, J.K. Gierse, J.J. McDonald, R.A. Stegeman, J.Y. Pak, D. Gildehaus, J.M. Miyashiro, T.D. Penning, K. Seibert, P.C. Isakson, W.C. Stallings, *Nature.*, **1996**, 384, 644.
[28] Prime, version 3.1, Schrödinger, LLC, New York, NY, 2012; Software available at http://www.schrodinger.com.
[29] R.A. Friesner, J.L. Banks, R.B. Murphy, T.A. Halgren, J.J. Klicic, D.T. Mainz, M.P. Repasky, E.H. Knoll, M. Shelley, J.K. Perry, D.E. Shaw, P. Francis, P.S. Shenkin, *J. Med. Chem.*, **2004**, 47, 1739.
[30] T.A. Halgren, R.B. Murphy, R.A. Friesner, H.S. Beard, L.L. Frye, W.T. Pollard, J.L. Banks, *J. Med. Chem.*, **2004**, 47, 1750.
[31] Maestro, version 9.3, Schrödinger LLC, New York, NY, 2012; Software available at http://www.schrodinger.com.
[32] LigPrep, version 2.5, Schrödinger LLC, New York, NY, 2012; Software available at http://www.schrodinger.com.
[33] S.G. Bhansali, V.M. Kulkarni, *Res. Rep. Med. Chem.* **2014**, 4, 1.
[34] G. Chang, W.C. Guida, W.C. Still, *J. Am. Chem. Soc.*, **1989**, 111, 4379.
[35] I. Kolossvary, W.C. Guida, *J. Am. Chem. Soc.*, **1996**, 118, 5011.
[36] VLife Molecular Design Suite 4.8.5, VLife Sciences Technologies Pvt. Ltd., Pune, India, 2004.
[37] J.R. Mann, R.N. Du Bois, Cyclooxygenase-2 and gastrointestinal cancer. *Cancer J.*, 10, 145.
[38] E.M. Behrens, *Autoimmun. Rev.*, **2008**, 7, 305.
[39] H.T. Wu, C.K. Chang, C.W. Tsao, Y.Z. Wen, Ling, S.M., Cheng, K.C., *Lab. Invest.,* 89, 362.